# Design, synthesis and biological evaluation of 6-substituted aminocarbonyl benzimidazole derivatives as nonpeptidic angiotensin II AT(1) receptor antagonists

**ARTICLE** *in* EUROPEAN JOURNAL OF MEDICINAL CHEMISTRY · MARCH 2012

Impact Factor: 3.45 · DOI: 10.1016/j.ejmech.2012.01.009 · Source: PubMed

European Journal of Medicinal Chemistry 49 (2012) 183–190

Contents lists available at SciVerse ScienceDirect

European Journal of Medicinal Chemistry

journal homepage: http://www.elsevier.com/locate/ejmech

Original article

# Design, synthesis and biological evaluation of 6-substituted aminocarbonyl benzimidazole derivatives as nonpeptidic angiotensin II $AT_1$ receptor antagonists

Jin-Liang Wang [a], Jun Zhang [a,*], Zhi-Ming Zhou [a,*], Zhi-Huai Li [a], Wei-Zhe Xue [a], Di Xu [a], Li-Ping Hao [a], Xiao-Feng Han [a], Fan Fei [a], Ting Liu [b], Ai-Hua Liang [b]

[a] R&D Center for Pharmaceuticals, School of Chemical Engineering & the Environment, Beijing Institute of Technology, 5 South Zhongguancun Street, Beijing 100081, China
[b] Institute of Chinese Materia Medica, China Academy of Chinese Medical Science, Beijing 100029, China

ARTICLE INFO

*Article history:*
Received 15 September 2011
Received in revised form
29 December 2011
Accepted 5 January 2012
Available online 17 January 2012

*Keywords:*
Angiotensin II $AT_1$ receptor antagonists
Aminocarbonyl benzimidazole
Hypertension

ABSTRACT

A series of 6-substituted aminocarbonyl benzimidazole derivatives were designed and synthesized as nonpeptidic angiotensin II $AT_1$ receptor antagonists. The preliminary pharmacological evaluation revealed nanomolar $AT_1$ receptor binding affinity and good $AT_1$ receptor selectivity over $AT_2$ receptor for all compounds of the series, a potent antagonistic activity in isolated rabbit aortic strip functional assay for compounds **6b**, **6d** and **6i** was also demonstrated. Furthermore, evaluation in spontaneous hypertensive rats and a preliminary toxicity evaluation showed that compound **6i** is an orally active $AT_1$ receptor antagonist with low toxicity.



## 1. Introduction

It is well known that the renin-angiotensin aldostenone system (RAAS) plays a key role in fluid/electrolyte homeostasis and blood pressure regulation [1,2]. Angiotensin II (Ang II) is an active octapeptide and a potent vasoconstrictor in the RAAS, which is produced in vivo from angiotensin I by the angiotensin-converting enzyme (ACE). Regulators of the RAAS have been found to be effective for the treatment of hypertension and congestive heart failure, and they continue to be one of the most active areas of drug discovery [3]. Among them, ACE inhibitors, such as captopril and enalapril, are useful in the treatment of hypertension, but may cause side effects, such as hypotension, angioedema and dry cough [4]. On the other hand, Ang II receptor antagonists directly block the effect of Ang II at the receptor level, without affecting kininase II-related factors, such as the bradykinin system. This provides a more specific way to the inhibition of the activity of the RAAS and has been considered a reliable alternative to inhibitors of ACE and renin [5].

Peptidic Ang II antagonists, such as saralasin, were found to reduce blood pressure in hypertensive patients with high renin levels. Unfortunately, long-term antihypertensive treatment with these drugs is not feasible because of their low oral bioavailability and short half-life [6]. The first nonpeptidic Ang II receptor antagonists, *N*-benzylimidazole-5-acetic acid derivatives, were firstly reported by the Takeda laboratories [7]. Since then, this imidazole lead has been developed into a series of potent, selective, and orally active $AT_1$ receptor antagonists. Losartan is the most widely used drug of this series, and numerous modifications to its chemical structure have generated a large number of Ang II antagonists [8–12], including candesartan, tasosartan, telmisartan, irbesartan and olmesartan (Fig. 1), all of which have been used clinically.

Data available from the literature [10] indicated that a benzimidazole scaffold was the most using core for good binding affinity with $AT_1$ receptor. Various substitutions in the benzimidazole nucleus at positions 5–7 have been studied for further modifications [9,10,13]. 4′-[[6-Carboxyl-4-methyl-2-propropyl-1*H*-benzimidazolyl]methyl]-2-biphenyl carboxylicacid (**1**, Fig. 2) was previously synthesized in our laboratory and exhibited moderate activity [14]. Thus we envisaged that the insertion of an aminocarbonyl moiety with lipophilic substituents at the 6-position of the benzimidazole nucleus as hydrogen-bond acceptor would produce significant effects on the binding affinities to the $AT_1$ receptor. In this paper, We describe the design, synthesis and biological evaluation of 6-substituted aminocarbonyl benzimidazole derivatives. A molecular modelling simulation was also performed to support our efforts in optimising the biological activity of the prepared compounds and obtaining a better understanding of the experimental results.

* Corresponding authors. Tel./fax: +86 10 68918982.
*E-mail addresses:* zhangjunbit@sina.com (J. Zhang), zzm@bit.edu.cn (Z.-M. Zhou).

0223-5234/$ – see front matter © 2012 Elsevier Masson SAS. All rights reserved.
doi:10.1016/j.ejmech.2012.01.009

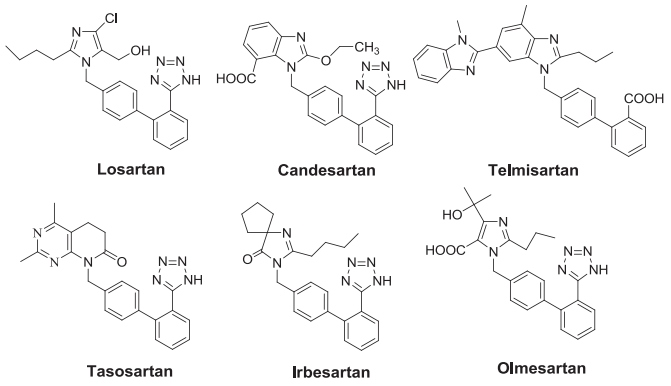


**Fig. 1.** Structures of several $AT_1$ receptor antagonists.

## 2. Chemistry

The target compounds **6a**–**6k** were synthesized according to the route described in Scheme 1, and the starting material 4-methyl-2-propyl-*1H*-benzimidazole6-carboxylic acid (**2**) used in this scheme was prepared from 3-methyl-4-nitrobenzoic acid according to the reported methods [14]. This compound was converted to the acyl chloride with thionyl dichloride under reflux conditions; the acyl chloride was then coupled with different amines to give the acylamide compounds **4a**–**4k** in 70–80% yield. The acylamides were then alkylated with methyl 4′-(bromomethyl) biphenyl-2-carboxylate using potassium *tert*-butoxide in DMF to give the corresponding products in yields of 70–90% yield. The last step, hydrolysis of **5a**–**5k** using aqueous sodium hydroxide in boiling MeOH, was accomplished with a greater than 70% yield.

All target compounds were identified by IR, $^1$H NMR, $^{13}$C NMR and HRMS. To provide confirmatory evidence on the regiochemistry of our target molecules, a Nuclear Overhauser Effect (NOE) experiment was conducted on one of the alkylation products, compound **5i** (Fig. 3). In DMSO-$d_6$, **5i** showed an NOE between the hydrogen of the methyl at C-4 ($\delta$ 2.59) and the proton at C-5 ($\delta$ 7.60), an NOE between the protons on the methylene adjacent to N-1 ($\delta$ 5.60) and the proton at C-7 ($\delta$ 7.95), and an NOE between the protons on the methylene adjacent to N-1 ($\delta$ 5.60) and the proton at the methylene adjacent to C-2. Furthermore, the structure of compound **5e** was confirmed by X-ray crystallography [15] (Fig. 4). Taken together, these indicate that the $N_1$ alkylation occurred rather than the $N_3$ alkylation.

## 3. Biological evaluation

The prepared compounds were evaluated for their in vitro Ang II receptor binding affinity in the competitive inhibition of [$^{125}$I] Ang II binding to the $AT_1$ and $AT_2$ receptors by a conventional ligand-binding assay as described previously [16]. The results are

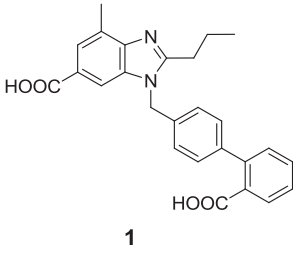

**1**

**Fig. 2.** Structure of compound **1**.

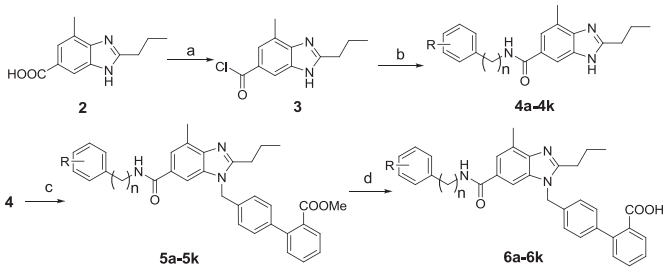


**Scheme 1.** Reagents and conditions: (a) thionyl dichloride, reflux, 3 h; (b) various substituted amines, $Et_3N$, DCM, rt, 6 h; (c) methyl-4′-bromomethylbiphenyl-2-carboxylic acid, t-BuOK, DMF, rt, 12 h; (d) NaOH, MeOH, $H_2O$, reflux, 3 h.

expressed as $IC_{50}$ values, which is the concentration of a compound that inhibits [$^{125}$I] Ang II binding to the receptor by 50%. The antagonistic activity of the more potent compounds (**6b**, **6d** and **6i**) were also investigated in vitro using the contractile response of isolated rabbit aortic strips in a functional assay [17]. Losartan was taken as a positive control drug in the assays. At last, the most potent compound **6i** was evaluated in an in vivo model.

Furthermore, a preliminary evaluation of toxicity to luminescent bacteria was performed on the prepared compounds according to the standard microtox test using luminescent bacteria, which is considered to be a useful tool, providing quick and reliable data [18].

## 4. Molecular modelling

In the molecular modelling simulation study, six clinically used sartans (Fig. 1) were selected as the training set, and the pharmacophore hypothesis generation was performed using the HipHop module of the Discovery Studio software [19]. Though the 3D structure of $AT_1$ receptor is unknown until now, an ideal pharmacophore hypothesis can be identified [20]. Accordingly, we used the method as a template, which represents the geometry of the receptor sites as a collection of functional groups in space. The fit values of the synthesised compounds were determined on the selected hypothesis of the $AT_1$ receptor antagonist using the best fit algorithm as described in the literature [21].

## 5. Results and discussion

As summarised in Table 1, the binding assay and the antagonistic activity results showed that all compounds displayed a certain extent of inhibition activity as expected. Most of compounds showed high selectivity for the $AT_1$ receptor over $AT_2$ receptor, given that the binding affinities were in the submicromolar range for the $AT_1$ receptor and in the micromolar range for the $AT_2$ receptor. Of all the synthesised compounds, compound **6i** was the most potent compound ($AT_1$ $IC_{50}$ = 1.3 nM, $AT_2$ $IC_{50}$ = 1400 nM), which exhibited almost the same binding affinity as the marketed $AT_1$ receptor antagonist telmisartan ($IC_{50}$ = 1.0 nM, 0.33 nM [23]),

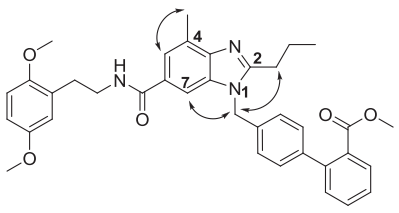

**Fig. 3.** NOESY of compound **5i**.

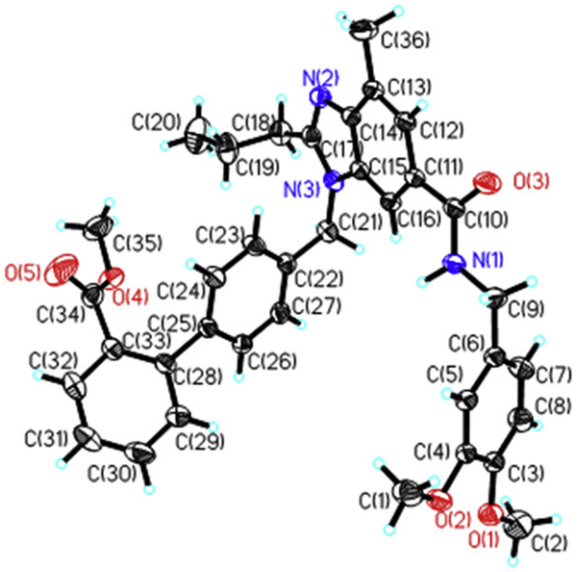


**Fig. 4.** Crystal structure of compound **5e**.

and about 12-fold the affinity of losartan ($IC_{50}$ = 16.2 nM, 150 nM [24], 6.7 nM [17,25]). The $pA_2$ 8.50 also shows that this compound contains more potent antagonist activity than the positive drug losartan ($pA_2$ = 7.9). Compounds **6b** ($AT_1$ $IC_{50}$ = 2.4 nM, $AT_2$ $IC_{50}$ = 1100 nM) and **6d** ($AT_1$ $IC_{50}$ = 4.3 nM, $AT_2$ $IC_{50}$ = 3600 nM) were also much more active than losartan. The $pA_2$ of compound **6b** and **6d** are 8.16 and 8.32 respectively, which are higher than that of losartan. In addition, compounds **6a**, **6e**, **6f** and **6h** showed the same activity level as losartan (10 nM < $AT_1$ $IC_{50}$ < 100 nM). These results suggested that both the length of aliphatic chains (which connect the acylamino moiety and the phenyl ring) and the substitution pattern on the aromatics played key roles in binding affinity.

Based on the results of in vitro AngII-binding assay and functional antagonism, **6i** were selected for further evaluation of in vivo models. When evaluated orally in conscious spontaneously hypertensive rats (SHR), compound **6i** at doses of 10 mg/kg significantly decreased blood pressure by more than 30 mmHg (Fig. 5), which is more efficacious than losartan.

In the molecular modelling simulation section, fit value indicates how well the chemical features in the molecule map the features in the pharmacophore [22]. The higher the fit value is, the more active a compound is. In this study, there are five features in the selected pharmacophore hypothesis, so the highest fit value is 5. Accordingly, the estimated activity could be classified according to the fit value as highly active (fit value > 4, +++), moderately active (2 < fit value<4, ++) and low active (fit value < 4, +). All synthesized compounds of this study were also classified according to the literature [21] by their activity as highly active (<100 nM, +++), moderately active (100–10000 nM, ++) and low active (>10000 nM, +). All highly active compounds were predicted correctly, only four moderately active compounds were predicted to be highly active. The results showed that despite these disparities, it could still to conclude that the pharmacophore hypothesis was reasonable. Furthermore, the molecular modelling simulation performed above reflected the interaction of ligands with the $AT_1$ receptor. Unexpectedly, it was the benzene ring in the phenylethyl, rather than the propyl at the 2-position of the benzimidazole ring that mapped onto the hydrophobic aliphatic feature. The same binding modality was also observed in the mapping of telmisartan with the pharmacophore (Fig. 6), in which it was the methyl in the second benzimidazole ring and not the propyl that mapped onto the hydrophobic aliphatic feature. However, in the case of losartan, it was the alkyl substituent that mapped onto the

**Table 1**
Fit values on the selected pharmacophore and experimental data of the target compounds.

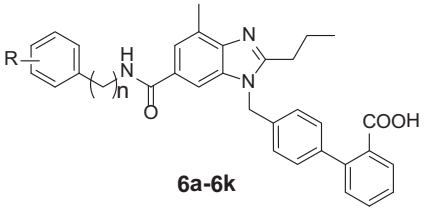


**6a-6k**

| No. | *n* | *R* | Fit value | $IC_{50}$(nM) | | est. act. scale[a] | act.($AT_1$R) scale[b] | $pA_2$ | $LC_{50}$ (mg $L^{-1}$) |
|---|---|---|---|---|---|---|---|---|---|
| | | | | $AT_1$ | $AT_2$ | | | | |
| **6a** | 1 | H | 4.78 | 52.5 | | +++ | +++ | | 78 |
| **6b** | 1 | 2-OMe | 4.70 | 2.4 | 1100 | +++ | +++ | 8.16 | >100[c] |
| **6c** | 1 | 3-OMe | 4.77 | 326 | >10,000 | +++ | ++ | | >100 |
| **6d** | 1 | 4-OMe | 4.87 | 4.3 | 3600 | +++ | +++ | 8.32 | >100 |
| **6e** | 1 | 3,4-di-OMe | 4.90 | 30.6 | >10,000 | +++ | +++ | | >100 |
| **6f** | 2 | 3-OMe | 4.90 | 30.8 | >10,000 | +++ | +++ | | 72 |
| **6g** | 2 | 4-OMe | 4.84 | 214 | 1500 | +++ | ++ | | >100 |
| **6h** | 2 | 3,4-di-OMe | 4.81 | 57.6 | 1200 | +++ | +++ | | >100 |
| **6i** | 2 | 2,5-di-OMe | 4.85 | 1.3 | 1400 | +++ | +++ | 8.50 | >100 |
| **6j** | 2 | 2-F | 4.71 | 106 | NT | +++ | ++ | | 65 |
| **6k** | 2 | 4-F | 4.91 | 198 | 1300 | +++ | ++ | | 89 |
| | | Losartan | 4.76 | 16.2 | >10,000 | +++ | +++ | | 210 |
| | | Telmisartan | 4.91 | 1.0 | | +++ | +++ | | >100 |

[a] Estimated activity scale: highly active (fit value > 4, +++), moderately active (2 < fit value < 4, ++) and low active (fit value < 4, +).
[b] Activity scale: highly active (<100 nM, +++), moderately active (100–10000 nM, ++) and low active (>10000 nM, +) [21].
[c] No $LC_{50}$ value could be determined because it did not produce more than 50% inhibition of luminescence of photobacterium phosphoreum at the saturated concentration level.

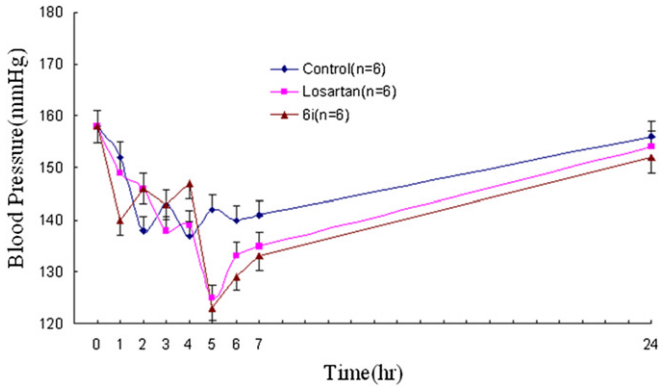


**Fig. 5.** Effects of **6i** and losartan (10 mg/kg po) on mean arterial pressure in conscious SHR after oral administration.

hydrophobic aliphatic feature (Fig. 7). This difference implied that the interaction modality of **6i**, like that of telmisartan, was not exactly the same as that of losartan. It is worth noting that the different interaction modalities of telmisartan and losartan have been reported in the literature [26] and were obtained through the docking of ligands with the homology modelled $AT_1$ receptor.

In the toxicity assay, the results revealed that the $LC_{50}$ value of most our synthetic compounds and telmisartan are higher than 100 mg $L^{-1}$, for they did not produce more than 50% inhibition of bacterial luminescence at the saturated concentration level. It is worth mentioning that the $LC_{50}$ value of losartan is 331 mg $L^{-1}$, which is almost the same as that (210 mg $L^{-1}$) obtained in another paper when the algae was used [27]. This experiment provide a choice to evaluate the preliminary toxicity of these compounds and the results showed that the toxicity of most compounds is as low as that of telmisartan.

## 6. Conclusions

In summary, a series of 6-substituted aminocarbonyl benzimidazole derivatives were designed and synthesized as nonpeptidic $AT_1$ receptor antagonists. Compounds **6i** was found to be the most potent $AT_1$-selective AII receptor antagonists with low toxicity, it could be used as lead compounds for the further design and synthesis of more potent nonpeptidic angiotensin II $AT_1$ receptor antagonists.

## 7. Experimental section

### 7.1. Chemistry

The melting points were determined on an XT-4A melting point apparatus and are uncorrected. All the target compounds were characterised by IR, $^1$H NMR, $^{13}$C NMR and HRMS. Infrared (IR) spectra were recorded on a PerkinElmer Spectrometer with KBr pellets, Nuclear magnetic resonance ($^1$H NMR and $^{13}$C NMR) spectra were recorded on a Bruker NMR spectrometer (400 MHz) using TMS as internal standard (chemical shift in ppm). High-resolution mass spectrums were recorded on a Fourier Transform Ion Cyclotron Resonance Mass Spectrometer. Silica gel column chromatography was performed with silica gel (200–300 mesh) and F254 precoated silica gel TLC plate.

#### 7.1.1. 4-Methyl-2-propyl-1H-benzimidazole-6-carboxylic chloride (*3*)

A mixture of 4-methyl-2-propyl-1*H*-benzimidazole-6-carboxylic acid (**2**) (5.2 g, 23.8 mmol) and thionyl dichloride (30 mL) was refluxed for 4 h, then thionyl dichloride was evaporated under reduced pressure to obtain off-white solid (5.64 g). It was used for the next step directly.

#### 7.1.2. General procedure for the preparation of acylamides (compound ***4a***–***4k***)

A mixture of amines (1.1 mmol), dichloromethane (30 mL) and triethylamine (0.3 g, 3 mmol) was placed in a three-necked bottle and cooled with ice. Then 4-methyl-2-propyl-1*H*-benzimidazole-6-carboxylic chloride (**3**) (0.24 g, 1 mmol) was added slowly. After the addition, the mixture was stirred at room temperature for 6 h. The white precipitate formed in the mixture was filtered, the filtrate was evaporated and the solid obtained was washed with saturated sodium bicarbonate and brine. The obtained acylamides was recrystallized from ethanol.

*7.1.2.1. N-Benzyl-[(4-methyl-2-propyl-1H-benzimidazole)-6-yl] amide (**4a**).* White solid (0.22 g, 72.3%), mp: 134–136 °C. $^1$H NMR (400 MHz, DMSO) $\delta$: 0.96 (t, $J$ = 7.2 Hz, 3H), 1.76 (m, 2H), 2.57 (s, 3H), 2.84 (t, $J$ = 7.1 Hz, 2H), 4.32 (s, 2H), 7.06–7.21 (m, 5H), 7.61 (s, 1H), 7.82 (s, 1H), 8.45 (s, 1H).

*7.1.2.2. N-(2-Methoxybenzyl)-[4-methyl-2-propyl-1H-benzimidazole)-6-yl]amide (**4b**).* White solid (0.26 g, 77.9%),mp: 129–131 °C. $^1$H NMR (400 MHz, DMSO) $\delta$: 0.94 (t, $J$ = 7.3 Hz, 3H), 1.76 (m, 2H), 2.56 (s, 3H), 2.83 (t, $J$ = 7.1 Hz, 2H), 3.47 (s, 3H), 4.45 (s, 2H), 7.09–7.31 (m, 4H), 7.57 (s, 1H), 7.88 (s, 1H), 8.48 (s, 1H).

*7.1.2.3. N-(3-Methoxybenzyl)-[4-methyl-2-propyl-1H-benzimidazole)-6-yl]amide (**4c**).* White solid (0.25 g, 74.8%), mp: 132–134 °C. $^1$H NMR (400 MHz, DMSO) $\delta$: 0.95 (t, $J$ = 7.2 Hz, 3H), 1.77 (m, 2H), 2.55 (s, 3H), 2.86 (t, $J$ = 7.1 Hz, 2H), 3.72 (s, 3H), 4.42 (s, 2H), 6.78–7.24 (m, 4H), 7.58 (s, 1H), 7.87 (s, 1H), 8.47 (s, 1H).

*7.1.2.4. N-(4-Methoxy benzyl)-[4-methyl-2-propyl-1H-benzimidazole)-6-yl]amide (**4d**).* White solid (0.24 g, 71.4%), mp: 133–135 °C. $^1$H NMR (400 MHz, DMSO) $\delta$: 0.94 (t, $J$ = 7.2 Hz, 3H), 1.79 (m, 2H), 2.56 (s, 3H), 2.87 (t, $J$ = 7.2 Hz, 2H), 3.78 (s, 3H), 4.47 (s, 2H), 6.82–7.29 (m, 4H), 7.55 (s, 1H), 7.82 (s, 1H), 8.46 (s, 1H).

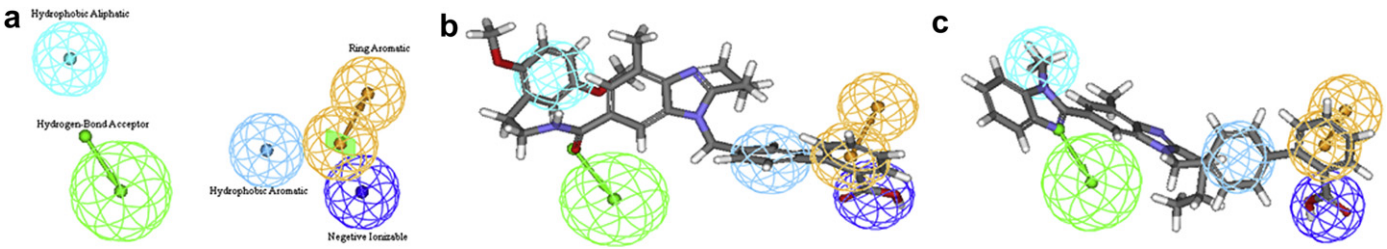


**Fig. 6.** (a) The selected pharmacophore hypothesis; (b) Mapping of **6i** with the selected hypothesis; (c) Mapping of telmisartan with the selected hypothesis.

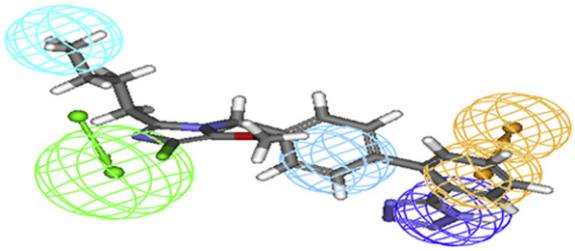

**Fig. 7.** Mapping of losartan with the selected hypothesis.

*7.1.2.5. N-(3,4-Dimethoxy benzyl) -[4-methyl-2-propyl-1H-benzimidazole)-6-yl]amide (**4e**).* White solid (0.28 g, 75.0%), mp: 128–130 °C. $^1$H NMR (400 MHz, DMSO) $\delta$: 0.81 (t, $J$ = 7.3 Hz, 3H), 1.72 (m, 2H), 2.50 (s, 3H), 2.81 (t, $J$ = 7.2 Hz, 2H), 3.71 (s, 3H), 3.79 (s, 3H), 4.43 (s, 2H), 6.99–7.01 (m, 3H), 7.68 (s, 1H), 7.81 (s, 1H).

*7.1.2.6. N-(3-Methoxyphenethyl)-[(4-methyl-2-propyl-1H-benzimidazole)-6-yl]amide (**4f**).* White solid (0.27 g, 75.7%), mp: 148–150 °C. $^1$H NMR (400 MHz, DMSO) $\delta$: 0.81 (t, $J$ = 7.2 Hz, 3H), 1.71 (m, 2H), 2.49 (s, 3H), 2.79 (t, $J$ = 7.2 Hz, 2H), 2.89 (t, $J$ = 7.2 Hz, 2H), 3.65 (m,2H), 3.77 (s, 3H), 6.77–7.20 (m, 4H), 7.67 (s, 1H), 7.78 (s, 1H).

*7.1.2.7. N-Benzyl-[(4-methyl-2-propyl-1H-benzimidazole)-6-yl] amide (**4g**).* White solid (0.27 g, 76.6%), mp: 149–151 °C. $^1$H NMR (400 MHz, DMSO) $\delta$: 0.98 (t, $J$ = 7.3 Hz, 3H), 1.81 (m, 2H), 2.57 (s, 3H), 2.77 (t, $J$ = 7.2 Hz, 2H), 2.88 (t, $J$ = 7.1 Hz, 2H), 3.40 (m, 2H), 3.67 (s, 3H), 6.84–7.32 (m, 4H), 7.45 (s, 1H), 7.84 (s, 1H).

*7.1.2.8. N-(3,4-Dimethoxyphenethyl)-[(4-methyl-2-propyl-1H-benzimidazole)-6-yl]amide (**4h**).* White solid (0.30 g, 78.7%), mp: 147–149 °C. $^1$H NMR (400 MHz, DMSO) $\delta$: 0.96 (t, $J$ = 7.2 Hz, 3H), 1.78 (m, 2H), 2.56 (s, 3H), 2.77 (t, $J$ = 7.2 Hz, 2H), 2.87 (t, $J$ = 7.2 Hz, 2H), 3.47 (m, 2H), 3.72 (s, 3H), 3.78 (s, 3H), 6.98–7.15 (m, 3H), 7.72 (s, 1H), 7.89 (s, 1H).

*7.1.2.9. N-(2,5-Dimethoxyphenethyl)-[(4-methyl-2-propyl-1H-benzimidazole)-6-yl]amide (**4i**).* White solid (0.28 g, 72.4%), mp: 145–147 °C. $^1$H NMR (400 MHz, DMSO) $\delta$: 0.95 (t, $J$ = 7.2 Hz, 3H), 1.76 (m, 2H), 2.55 (s, 3H), 2.78 (t, $J$ = 7.2 Hz, 2H), 2.86 (t, $J$ = 7.2 Hz, 2H), 3.48 (m, 2H), 3.70 (s, 3H), 3.76 (s, 3H), 6.94–7.12 (m, 3H), 7.70 (s, 1H), 7.86 (s, 1H).

*7.1.2.10. N-(2-Fluorophenethyl-[(4-methyl-2-propyl-1H-benzimidazole)-6-yl]amide (**4j**).* White solid (0.26 g, 76.3%), mp: 133–135 °C. $^1$H NMR (400 MHz, DMSO) $\delta$: 0.95 (t, $J$ = 7.2 Hz, 3H), 1.67 (m, 2H), 2.55 (s, 3H), 2.75 (t, $J$ = 7.2 Hz, 2H), 2.86 (t, $J$ = 7.2 Hz, 2H), 3.53 (m, 2H), 6.93–7.25 (m, 4H), 7.47 (s, 1H), 7.82 (s, 1H).

*7.1.2.11. N-(4-Fluorophenethyl-[(4-methyl-2-propyl-1H-benzimidazole)-6-yl]amide (**4k**).* White solid (0.25 g, 74.4%), mp: 137–139 °C. $^1$H NMR (400 MHz, DMSO) $\delta$: 0.96 (t, $J$ = 7.2 Hz, 3H), 1.69 (m, 2H), 2.56 (s, 3H), 2.78 (t, $J$ = 7.3 Hz, 2H), 2.87 (t, $J$ = 7.2 Hz, 2H), 3.56 (m, 2H), 6.97–7.23 (m, 4H), 7.46 (s, 1H), 7.84 (s, 1H).

*7.1.3. General procedure for the preparation of alkylated products (compound **5a**–**5k**)*

A mixture of amide compound (one of compound in **4a**–**4k**) (2 mmol) and 3 mL DMF was placed in a three-necked bottle and-cooled with ice, then potassium tert-butoxide 354 mg (3 mmol) was added. After stirring at the same temperature for 30 min, methyl-4′-bromomethyl-2-biphenylcarboxylic acid 610 mg (2.1 mmol) was added. After addition of all reagents, the ice bath was removed, and the reaction mixture was stirred overnight. The mixture was poured into 30 mL water then extracted with ethyl ester. The extract was washed with water and dried ($MgSO_4$). After the evaporation of the solvent in vacuo, the residue was purified by flash column chromatography.

*7.1.3.1. Methyl 4′-[(6-benzylaminocarboxyl-4-methyl-2-propyl-1H-benzimidazolyl)methyl]biphenyl-2- carboxylate (**5a**).* White solid (801 mg, 75.3%), mp: 122–124 °C. $^1$H NMR (400 MHz, $CDCl_3$) $\delta$: 0.98 (t, $J$ = 7.4 Hz, 3H), 1.80 (m, 2H), 2.65 (s, 3H), 2.84 (t, $J$ = 7.6 Hz, 2H), 3.58 (s, 3H), 4.59 (t, $J$ = 5.6 Hz, 2H), 5.33 (s, 2H), 6.99–7.80 (m, 15H), 8.44 (s, 1H); ESIMS($m/z$): 532.3$(M + H)^+$.

*7.1.3.2. Methyl 4′-[[6-(2′-methoxy)benzylaminocarboxyl-4-methyl-2-propyl-1H-benzimidazolyl]methyl]biphenyl-2- carboxylate (**5b**).* White solid (940 mg, 83.6%), mp: 163–164 °C. $^1$H NMR (400 MHz, $CDCl_3$) $\delta$: 0.97 (t, $J$ = 7.2 Hz, 3H), 1.74 (m, 2H), 2.55 (s, 3H), 2.84 (t, $J$ = 7.6 Hz, 2H), 3.47 (s, 3H), 3.69 (s, 3H), 4.45 (s, 2H), 5.55 (s, 2H), 7.12–7.86 (m, 14H), 8.45 (s, 1H); ESIMS($m/z$):562.3$(M + H)^+$.

*7.1.3.3. Methyl 4′-[[6-(3′-methoxy)benzylaminocarboxyl-4-methyl-2-propyl-1H-benzimidazolyl]methyl]biphenyl-2- carboxylate (**5c**).* White solid (1007 mg, 89.7%), mp: 124–125 °C. $^1$H NMR (400 MHz, $CDCl_3$) $\delta$: 0.95 (t, $J$ = 7.2 Hz, 3H), 1.76 (m, 2H), 2.56 (s, 3H), 2.79 (t, $J$ = 7.2 Hz, 2H), 3.68 (s, 3H), 3.73 (s, 3H), 4.41 (s, 2H), 5.56 (s, 2H), 7.08–7.92 (m, 14H), 8.43 (s, 1H); ESIMS($m/z$): 562.3$(M + H)^+$.

*7.1.3.4. Methyl 4′-[[6-(4′-methoxy)benzylaminocarboxyl-4-methyl-2-propyl-1H-benzimidazolyl]methyl]biphenyl-2- carboxylate (**5d**).* White solid (1028 mg, 91.5%), mp: 147–148 °C. $^1$H NMR (400 MHz, $CDCl_3$) $\delta$: 0.96 (t, $J$ = 7.2 Hz, 3H), 1.75 (m, 2H), 2.55 (s, 3H), 2.79 (t, $J$ = 7.2 Hz, 2H), 3.69 (s, 3H), 3.77 (s, 3H), 4.46 (s, 2H), 5.56 (s, 2H), 7.09–7.90 (m, 14H), 8.44 (s, 1H); ESIMS($m/z$): 562.3$(M + H)^+$.

*7.1.3.5. Methyl 4′-[[6-(3′,4′-dimethoxy)benzylaminocarboxyl-4-methyl-2-propyl-1H-benzimidazolyl]methyl]biphenyl-2- carboxylate (**5e**).* White solid (927 mg, 78.3%), mp: 126–127 °C. $^1$H NMR (400 MHz, $CDCl_3$) $\delta$: 0.96 (t, $J$ = 7.2 Hz, 3H), 1.75 (m, 2H), 2.55 (s, 3H), 2.79 (t, $J$ = 7.2 Hz, 2H), 3.67 (s, 3H), 3.72 (s, 3H), 3.80 (s, 3H), 4.42 (s, 2H), 5.55 (s, 2H), 7.07–7.93 (m, 13H), 8.43 (s, 1H) ; ESIMS($m/z$): 592.3$(M + H)^+$.

*7.1.3.6. Methyl 4′-[[6-(3′-methoxy)phenethylaminocarboxyl-4-methyl-2-propyl-1H-benzimidazolyl]methyl]biphenyl-2- carboxylate (**5f**).* White solid (832 mg, 72.3%), mp: 110–112 °C. $^1$H NMR (400 MHz, $CDCl_3$) $\delta$: 1.02 (t, $J$ = 7.4 Hz, 3H), 1.80–1.86 (m, 2H), 2.68 (s, 3H), 2.87–2.92 (m, 4H), 3.61 (s, 3H), 3.67–3.72 (m, 2H), 3.77 (s, 3H), 5.40 (s, 2H), 6.21 ( s, 1H ) , 6.77–7.62 (m, 13H), 7.81 (d, $J$ = 0.8 Hz, 1H); ESIMS ($m/z$): 576.3$(M + H)^+$.

*7.1.3.7. Methyl 4′-[[6-(4′-methoxy)phenethylaminocarboxyl-4-methyl-2-propyl-1H-benzimidazolyl]methyl]biphenyl-2-carboxylate (**5g**).* White solid (931 mg, 81.0%), mp: 113–114 °C. $^1$H NMR (400 MHz, $CDCl_3$) $\delta$: 0.97 (t, $J$ = 7.2 Hz, 3H), 1.73 (m, 2H), 2.56 (s, 3H), 2.78 (t, $J$ = 7.2 Hz, 2H), 2.87 (t, $J$ = 7.1 Hz, 2H), 3.47 (m, 2H), 3.58 (s, 3H), 3.69 (s, 3H), 5.56 (s, 2H), 7.10–7.90 (m, 14H), 8.45 (s, 1H); ESIMS ($m/z$): 576.3$(M + H)^+$.

*7.1.3.8. Methyl 4′-[[6-(3′,4′-dimethoxy)phenethylaminocar-boxyl-4-methyl-2-propyl-1H-benzimidazolyl]methyl] biphenyl-2-carboxylate (**5h**).* White solid (1016 mg, 84.0%), mp: 145–146 °C. $^1$H NMR (400 MHz, $CDCl_3$) $\delta$: 0.94 (t, $J$ = 7.2 Hz, 3H), 1.77 (m, 2H), 2.56 (s, 3H), 2.77 (t, $J$ = 7.2 Hz, 2H), 2.87 (t, $J$ = 7.2 Hz, 2H), 3.49 (m, 2H), 3.61 (s, 3H), 3.73 (s, 3H), 3.79 (s, 3H), 5.56 (s, 2H), 7.10–7.91 (m, 13H), 8.44 (s, 1H); ESIMS ($m/z$): 606.3$(M + H)^+$.

*7.1.3.9. Methyl 4′-[[6-(2′,5′-dimethoxy)phenethylaminocarboxyl-4-methyl-2-propyl-1H-benzimidazolyl]methyl] biphenyl-2- carboxylate*

(**5i**). White solid (1098 mg, 90.7%), mp: 130–132 °C. $^1$H NMR (400 MHz, $CDCl_3$) δ: 0.96 (t, $J$ = 7.3 Hz, 3H), 1.75 (m, 2H), 2.55 (s, 3H), 2.80 (t, $J$ = 7.2 Hz, 2H), 2.85 (t, $J$ = 7.2 Hz, 2H), 3.48 (m, 2H), 3.60 (s, 3H), 3.71 (s, 3H), 3.77 (s, 3H), 5.55 (s, 2H), 7.07–7.87 (m, 13H), 8.43 (s, 1H); ESIMS (*m/z*): 606.3$(M + H)^+$.

*7.1.3.10. Methyl 4′-[[6-(2′-fluoro)phenethylaminocarboxyl-4-methyl-2-propyl-1H-benzimidazolyl]methyl]biphenyl-2-carboxylate (**5j**).* White solid (784 mg, 69.6%), mp: 140–142 °C. $^1$H NMR (400 MHz, $CDCl_3$) δ: 0.95 (t, $J$ = 7.2 Hz, 3H), 1.74 (m, 2H), 2.55 (s, 3H), 2.79 (t, $J$ = 7.2 Hz, 2H), 2.85 (t, $J$ = 7.1 Hz, 2H), 3.53 (m, 2H), 3.66 (s, 3H), 5.55 (s, 2H), 7.13–7.85 (m, 14H), 8.44 (s, 1H); ESIMS(*m/z*): 564.3$(M + H)^+$.

*7.1.3.11. Methyl 4′-[[6-(4′-fluoro)phenethylaminocarboxyl-4-methyl-2-propyl-1H-benzimidazolyl]methyl]biphenyl-2-carboxylate (**5k**).* White solid (953 mg, 84.7%), mp: 157–158 °C. $^1$H NMR (400 MHz, $CDCl_3$) δ: 0.96 (t, $J$ = 7.2 Hz, 3H), 1.73 (m, 2H), 2.56 (s, 3H), 2.78 (t, $J$ = 7.2 Hz, 2H), 2.86 (t, $J$ = 7.2 Hz, 2H), 3.56 (m, 2H), 3.69 (s, 3H), 5.55 (s, 2H), 7.08–7.96 (m, 14H), 8.45 (s, 1H) ; ESIMS(*m/z*): 564.3$(M + H)^+$.

*7.1.4. General procedure for the preparation of target compounds (compound **6a**–**6k**)*

Alkylated products (0.4 mmol) were added into a bottle, and then 5 mL methanol and 2 mL of 2 N sodium hydroxide solution were added. The mixture was heated and refluxed for 3 h. After the completion of the hydrolysis, the mixture was evaporated to remove methanol. Then the mixture system was acidified with 2N aqueous hydrochloride to pH 6, and the white precipitate was filtered and dried.

*7.1.4.1. 4′-[(6-benzylaminocarboxyl-4-methyl-2-propyl-1H-benzimidazolyl)methyl]-2-biphenyl carboxylic acid (**6a**).* White solid (147 mg, 71.2%), mp 266–268 °C, IR (KBr): 3025, 2951, 1698, 1520, 1271, 776. $^1$H NMR (400 MHz,DMSO-$d_6$) δ: 0.96 (t, $J$ = 7.2 Hz, 3H), 1.78 (m, 2H), 2.51 (s, 3H), 2.84 (t, $J$ = 7.3 Hz, 2H), 4.47 (s, 2H), 5.54 (s, 2H), 7.05–7.95 (m, 15H), 8.97 (s, 1H). HRMS: calcd for $C_{33}H_{31}N_3O_3$ $(MH^+)$518.2365, found 518.2359.

*7.1.4.2. 4′-[(4-Methyl-6-2′-methoxy-benzylaminocarboxyl-2-propyl-1H-benzimidazolyl)methyl]-2-biphenyl carboxylic acid (**6b**).* White solid (162 mg, 73.9%), mp 243–245 °C, IR (KBr): 3395, 1655, 1598, 1540, 1490, 1459, 1358, 1243, 1122, 1026, 870, 818, 764. $^1$H NMR (400 MHz, DMSO-$d_6$) δ: 0.97 (t, $J$ = 7.2 Hz, 3H), 1.74 (m, 2H), 2.55 (s, 3H), 2.78 (t, $J$ = 7.2 Hz, 2H), 3.47 (s, 3H), 4.45 (s, 2H), 5.56 (s, 2H), 7.12–7.86 (m, 14H), 8.45 (s, 1H), 12.72 (br, 1H). $^{13}$C NMR (100 MHz, DMSO-$d_6$) δ: 13.98, 16.64, 18.71, 20.69, 28.90, 46.01, 55.48, 56.18, 107.56, 110.58, 110.25, 121.30, 126.19, 127.27, 127.50, 127.61, 127.97, 128.12, 128.89, 129.24, 130.60, 131.00, 132.36, 134.85, 136.08, 140.22, 140.57, 143.98, 156.71, 156.77, 166.92, 169.62. HRMS: calcd for $C_{34}H_{34}N_3O_4(MH^+)$ 548.2544, found 548.2533.

*7.1.4.3. 4′-[(4-Methyl-6-3′-methoxybenzylaminocarboxyl-2-propyl-1H-benzimidazolyl)methyl]-2-biphenylcarboxylic acid (**6c**).* White solid (181 mg, 82.8%), mp 228–229 °C, IR (KBr): 3375, 1648, 1598, 1534, 1487, 1456, 1349, 1270, 1047, 853, 765. $^1$H NMR (400 MHz, DMSO-$d_6$) δ: 0.95 (t, $J$ = 7.2 Hz, 3H), 1.76 (m, 2H), 2.56 (s, 3H), 2.79 (t, $J$ = 7.2 Hz, 2H), 3.73 (s, 3H), 4.41 (s, 2H), 5.55 (s, 2H), 7.08–7.92 (m, 14H), 8.43 (s, 1H), 12.71 (br, 1H). $^{13}$C NMR (100 MHz, DMSO-$d_6$) δ: 13.98, 16.64, 18.71, 20.68, 28.89, 42.80, 46.01, 55.11, 56.18, 107.55, 112.13, 113.18, 119.59, 121.26, 126.18, 127.47, 127.63, 128.06, 128.89, 129.24, 129.47, 130.60, 131.00, 132.35, 134.85, 136.06, 140.22, 140.58, 141.67, 144.00, 156.80, 159.44, 166.78, 169.63. HRMS: calcd for $C_{34}H_{34}N_3O_4$ $(MH^+)$ 548.2544, found 548.2531.

*7.1.4.4. 4′-[(4-Methyl-6-4′-methoxybenzylaminocarboxyl-2-propyl-1H-benzimidazolyl)methyl]-2-biphenylcarboxylic acid (**6d**).* White solid (174 mg, 79.3%), mp >250 °C, IR (KBr): 3357, 1652, 1593, 1533, 1511, 1454, 1293, 1245, 1041, 880, 818, 756. $^1$H NMR (400 MHz, DMSO-$d_6$) δ: 0.96 (t, $J$ = 7.2 Hz, 3H), 1.75 (m, 2H), 2.55 (s, 3H), 2.79 (t, $J$ = 7.2 Hz, 2H), 3.77 (s, 3H), 4.46 (s, 2H), 5.56 (s, 2H), 7.09–7.90 (m, 14H), 8.44 (s, 1H), 12.72 (br, 1H). $^{13}$C NMR (100 MHz, DMSO-$d_6$) δ: 13.98, 16.63, 20.67, 28.89, 42.30, 46.00, 55.20, 56.18, 107.51, 113.81, 121.25, 126.17, 127.47, 127.58, 128.14, 128.79, 128.89, 129.24, 130.69, 131.00, 132.03, 132.36, 134.85, 136.07, 140.21, 140.57, 143.95, 156.76, 158.31, 166.64, 169.63. HRMS: calcd for $C_{34}H_{34}N_3O_4$ $(MH^+)$ 548.2544, found 548.2533.

*7.1.4.5. 4′-[(6-3′,4′-Dimethoxybenzylaminocarboxyl-4-methyl-2-propyl-1H-benzimidazolyl)methyl]-2-biphenyl carboxylic acid (**6e**).* White solid (166 mg, 71.7%), mp >250 °C, IR (KBr): 3346, 1653, 1593, 1513, 1462, 1418, 1257, 1215, 1149, 1034, 1012, 814, 754. $^1$H NMR (400 MHz, DMSO-$d_6$) δ: 0.96 (t, $J$ = 7.2 Hz, 3H), 1.75 (m, 2H), 2.55 (s, 3H), 2.79 (t, $J$ = 7.2 Hz, 2H), 3.72 (s, 3H), 3.80 (s, 3H), 4.42 (s, 2H), 5.55 (s, 2H), 7.07–7.93 (m, 13H), 8.43 (s, 1H), 12.72 (br, 1H). HRMS: calcd for $C_{35}H_{36}N_3O_5$ $(MH^+)$ 578.2650, found 578.2638.

*7.1.4.6. 4′-[[4-Methyl-6-(2-(3′-methoxyphenethylamino)carboxyl-2-propyl-1H-benzimidazolyl]methyl]-2-biphenyl carboxylic acid (**6f**).* White solid (197 mg, 87.8%), mp 239–240 °C, IR (KBr): 3368, 1654, 1593, 1544, 1451, 1347, 1279, 1155, 1042, 875, 763. $^1$H NMR (400 MHz, DMSO-$d_6$) δ: 0.96(t, $J$ = 7.4 Hz, 3H), 1.72–1.82 (m, 2H), 2.56 (s, 3H), 2.80–2.86(m, 4H), 3.45–3.50 (m, 2H), 3.70 (s, 3H), 5.56 (s, 2H), 6.75–6.81 (m, 3H), 7.09–7.87(m, 11H), 8.42 (t, $J$ = 5.4 Hz, 1H), 12.72 (s, 1H). $^{13}$C NMR (100 MHz, DMSO-$d_6$) δ: 13.98, 16.64, 20.69, 28.88, 35.41, 45.99, 55.00, 56.18, 107.39, 111.73, 114.39, 121.06, 121.16, 126.17, 127.48, 127.53, 128.39, 128.90, 129.25, 129.47, 130.60, 131.01, 132.35, 136.06, 140.23, 140.58, 141.37, 143.87, 156.70, 159.43, 166.75, 169.63.HRMS: calcd for $C_{35}H_{36}N_3O_4$ $(MH^+)$562.2700, found 562.2690.

*7.1.4.7. 4′-[[4-Methyl-6-(2-(4′-methoxyphenethylamino)carboxyl-2-propyl-1H-benzimidazolyl]methyl]-2-biphenyl carboxylic acid (**6g**).* White solid (186 mg, 82.7%), mp 243–244 °C, IR (KBr): 3377, 1673, 1644, 1599, 1533, 1511, 1483, 1455, 1349, 1269, 1243, 1029, 820, 761. $^1$H NMR (400 MHz, DMSO-$d_6$) δ: 0.97 (t, $J$ = 7.2 Hz, 3H), 1.73 (m, 2H), 2.56 (s, 3H), 2.78 (t, $J$ = 7.2 Hz, 2H) 2.87 (t, $J$ = 7.1 Hz, 2H), 3.47 (m, 2H), 3.69 (s, 3H), 5.55 (s, 2H), 7.10–7.90(m, 14H), 8.45 (s, 1H), 12.72 (br, 1H). $^{13}$C NMR (100 MHz, DMSO-$d_6$) δ: ; 13.98, 16.65, 18.72, 20.69, 28.88, 34.54, 41.40, 46.00, 55.11, 107.39, 113.92, 121.16 , 126.17, 127.47, 127.52, 128.40, 128.90, 129.25, 129.73, 130.60, 131.00, 131.65, 132.36, 134.80, 136.06, 140.23, 140.57, 143.87, 156.69, 157.81, 166.70, 169.63. HRMS: calcd for $C_{35}H_{36}N_3O_4$ $(MH^+)$562.2700, found 562.2691.

*7.1.4.8. 4′-[[4-Methyl-6-(2-(3′,4′-dimethoxy)phenethylamino) carboxyl-2-propyl-1H-benzimidazolyl]methyl]-2-biphenyl carboxylic acid (**6h**).* White solid (178 mg, 75.3%), mp 240–241 °C, IR (KBr): 3388, 1679, 1643, 1597, 1544, 1513, 1461, 1350, 1272, 1153, 1035, 889, 819, 760. $^1$H NMR (400 MHz, DMSO-$d_6$) δ: 0.94 (t, $J$ = 7.2 Hz, 3H), 1.77 (m, 2H), 2.56 (s, 3H), 2.77 (t, $J$ = 7.2 Hz, 2H), 2.87 (t, $J$ = 7.2 Hz, 2H), 3.49 (m, 2H), 3.73 (s, 3H), 3.79 (s, 3H), 5.55 (s, 2H), 7.10–7.91 (m, 13H), 8.44 (s, 1H), 12.72 (br, 1H). $^{13}$C NMR (100 MHz, DMSO-$d_6$) δ: 13.98, 16.64, 18.72, 20.69, 28.89, 34.93, 41.32, 46.00, 55.47, 55.66, 56.18, 107.38, 112.09, 112.74, 120.62, 121.16, 126.16, 127.48, 127.52, 128.43, 128.90, 129.26, 130.61, 131.01, 132.29, 132.35, 134.41, 136.06, 140.23, 140.58, 143.86, 147.37, 148.76, 156.70, 166.72, 169.63. HRMS: calcd for $C_{36}H_{38}N_3O_5(MH^+)$ 592.2806, found 592.2793.

*7.1.4.9. 4′-[[4-Methyl-6-(2-(2′,5′-dimethoxy)phenethylamino) carboxyl-2-propyl-1H-benzimidazolyl]methyl]-2-biphenyl carboxylic*

*acid (**6i**).* White solid (194 mg, 82%), mp 231–233 °C, IR (KBr): 3361, 1654, 1597, 1536, 1501, 1465, 1355, 1291, 1244, 1039,809, 764. $^1$H NMR (400 MHz, DMSO-$d_6$) $\delta$: 0.96 (t, $J$ = 7.3 Hz, 3H), 1.75 (m, 2H), 2.55(s, 3H), 2.80 (t, $J$ = 7.2 Hz, 2H), 2.85 (t, $J$ = 7.2 Hz, 2H), 3.48 (m, 2H), 3.71(s, 3H), 3.77 (s, 3H), 5.56 (s, 2H), 7.07–7.87 (m, 13H), 8.43 (s, 1H), 12.73(br, 1H). $^{13}$C NMR (100 MHz, DMSO-$d_6$) $\delta$:13.98, 16.64, 18.71, 20.68, 28.89, 30.09, 45.98, 55.38, 55.95, 56.18, 107.35, 111.73, 111.80, 116.38, 121.19, 126.16, 127.48, 128.44, 128.73, 128.90, 129.25, 130.60, 131.00, 132.36, 134.80, 136.07, 140.22, 140.58, 143.84, 151.55, 153.14, 156.67, 166.70, 169.63. HRMS: calcd for $C_{36}H_{38}N_3O_5$ ($MH^+$) 592.2806, found 592.2795.

*7.1.4.10. 4′-[[6-(2-(2′-Fluoro)phenethylamino)carboxyl-4-methyl-2-propyl-1H-benzimidazolyl]methyl]-2-biphenyl carboxylic acid (**6j**).* White solid (169 mg, 76.9%), mp 233–234 °C, IR (KBr): 3404, 1652, 1600, 1545, 1489, 1457, 1352, 1266, 1218, 1137, 822, 757. $^1$H NMR (400 MHz, DMSO-$d_6$) $\delta$: 0.95 (t, $J$ = 7.2 Hz, 3H), 1.74 (m, 2H), 2.55 (s, 3H), 2.79 (t, $J$ = 7.2 Hz, 2H), 2.85 (t, $J$ = 7.1 Hz, 2H), 3.53 (m, 2H), 5.55 (s, 2H), 7.13–7.85 (m, 14H), 8.44 (s, 1H), 12.72 (br, 1H). $^{13}$C NMR (100 MHz, DMSO-$d_6$) $\delta$: 13.98, 16.65, 18.72, 20.70, 28.88, 46.00, 56.18, 107.40, 115.15, 115.37, 121.16, 124.48, 124.52, 126.17, 126.23, 126.39, 127.48, 127.53, 128.31, 128.37, 128.45, 128.90, 129.25, 130.60, 131.00, 131.35, 131,40, 132.38, 134.79, 136.05, 140.23, 140.57, 143.90, 156.71, 159.69, 162.11, 166.78, 169.64. HRMS: calcd for $C_{34}H_{33}FN_3O_3$($MH^+$) 550.2501, found 550.2489.

*7.1.4.11. 4′-[[6-(2-(4′-Fluoro)phenethylamino)carboxyl-4-methyl-2-propyl-1H-benzimidazolyl]methyl]-2-biphenyl carboxylic acid (**6k**).* White solid (174 mg, 79.4%), mp >250 °C, IR (KBr): 3386, 1645, 1598, 1573, 1508, 1455, 1351, 1272, 1217, 1157, 1083, 875, 820, 716. $^1$H NMR (400 MHz, DMSO-$d_6$) $\delta$: 0.96 (t, $J$ = 7.2 Hz, 3H), 1.73 (m, 2H), 2.56 (s, 3H), 2.78 (t, $J$ = 7.2 Hz, 2H), 2.86 (t, $J$ = 7.2 Hz, 2H), 3.56 (m, 2H), 5.56 (s, 2H), 7.08–7.96 (m, 14H), 8.45 (s, 1H), 12.71 (br, 1H). $^{13}$C NMR (100 MHz, DMSO-$d_6$) $\delta$: 13.98, 16.65, 18.72, 20.70, 28.88, 34.50, 46.00, 56.18, 107.40, 115.02, 115.23, 121.15, 126.16, 127.48, 127.55, 128.34, 128.90, 129.26, 130.52, 130.60, 131.00, 132.37, 134.80, 135.91, 135.94, 136.05, 140.24, 140.57, 143.89, 156.72, 159.76, 162.17, 166.77, 169.63. HRMS: calcd for $C_{34}H_{33}FN_3O_3$ ($MH^+$)550.2501, found 550.2490.

### 7.2. Procedure for receptor binding assay

The $AT_1$ receptor binding assay was carried out by competitive displacement of the binding of [$^{125}$I] Sar$^1$ Ile$^8$-Ang II with angiotensin $AT_1$ receptor as described previously [16]. Each 180 μL incubate contained the following: [$^{125}$I] Sar$^1$ Ile$^8$-Ang II (25pM), $AT_1$($AT_2$) receptor (25 μg) and standard or test compounds. The binding was performed at 37 °C for 180 min in 96-well filtration plates (Costar, USA) and was terminated by rapid vacuum filtration using a vacuum device; dried filters disks were punched out and counted in a gamma counter. $IC_{50}$ values were estimated from the linear portion of the competition curves.

### 7.3. Procedure for angiotensin II receptor functional antagonism in rabbit aorta strips

Japanese White Rabbits (2–3 kg body weight, Vitalriver Company, China) were killed by cervical dislocation, after a slight anesthesia with 20% Urethane solution. The thoracic aorta was carefully dissected out, placed in ice-cold Krebs-Henseleit solution of the following composition (mM): NaCl 118; KCl 4.7; $KH_2PO_4$ 1.2; $MgSO_4{\cdot}7H_2O$ 1.17; $CaCl_2{\cdot}2H_2O$ 2.5; $NaHCO_3$ 25; glucose 11.1 [28]. It was cut into helical strips 3–4 mm wide and 15–20 mm long. These strips were mounted in 10-mL tissue baths, the tissue baths were kept at 37 °C and aerated with 95% $O_2$ and 5% $CO_2$. Each strip was connected to a force transducer, the changes in isometric tension were recorded by a four-channel recorder (Medlab-U/4c501, China). The tissues were allowed to equilibrate for 1 h and were washed every 15 min. At the beginning of the experiment, a 67 mM KCl solution was administered to check the sensitivity of the preparations as well as to determine their maximal contractile response. After 30 min washout, test substances or their respective vehicles were added. Sixty minutes later, cumulative concentration–response curves of angiotensin II were obtained. Only one curve was obtained from each strip, and the contractile response was expressed as percentage (%) of the maximal contraction achieved with KCl. The $pA_2$ values were calculated using Schild's plot [29]. Antagonist potency was evaluated by the estimation of $pA_2$ values.

### 7.4. Procedure for oral activity in the spontaneously hypertensive rats (SHR)

Male SHR, 19–21 weeks old. Six animals served as controls. They received vehicle (10 mL/kg). Hypertensive animals were divided into two groups ($n$ = 6). Group 1 received losartan (standard drug: 10 mg/kg), group 2 was given the same doses of the tested compound **6i**. Both the vehicle and test compound were given by oral administration [30]. Blood pressure and heart rate were measured by tail plethysmography (BP-98A, Softron, Japan) after a warming period in unanesthetized rats. The BP measurements required only a few minutes per individual rat. All data were expressed as means ± SEM [13c].

### 7.5. Procedure for preliminary toxicity evaluation

The preliminary toxicity evaluation was performed on a water toxicity analyser (BHP 9511, Beijing Hamamatsu Inc.) by the inhibition of Photobacterium phosphoreum (T3 mutation), which was supplied by the Institute of Soil Science, Academia Sinica, Nanjing P. R. China in the form of a freeze dried powder. For each test, a serial dilution of the compounds was prepared in 2% saline water according to the pre-test. In addition, a series of saline solutions containing $10^6$ colony units of Photobacterium phosphoreum was prepared in glass cuvettes by pipetting 10 mL of the reconstituted bacterial suspension into 500 mL of a 2% saline solution. These solutions were incubated for 15 min and measured. The toxicity of the treated compounds was recorded after 15 min of exposure to the tested sample. The results of the Microtox test are expressed in terms of $LC_{50}$ values. $LC_{50}$ is the concentration in water which inhibits 50% of a test batch of Photobacterium phosphoreum as exemplified by compound **6i** and **6j** in Fig. 8. The lower the $LC_{50}$ value is, the greater the toxicity of the sample is [31].

### 7.6. Molecular modelling experiments

Molecular modelling studies were performed using a Silicon Graphics desktop (SGI) Fuel work station. The training set was selected as described above, and the pharmacophore model for $AT_1$ receptor antagonists was generated using the HipHop module in Discovery Studio, version 2.0, from Accelrys Inc. Molecules were built in a 3D window, and conformational models for each molecule were generated using the diverse conformation module. Then the resulting sd files were used for common features hypothesis generation using the HipHop module by default. Through these experiments, we specified the features that are crucial for binding with Ang II receptor, in agreement with the literature [20,21].

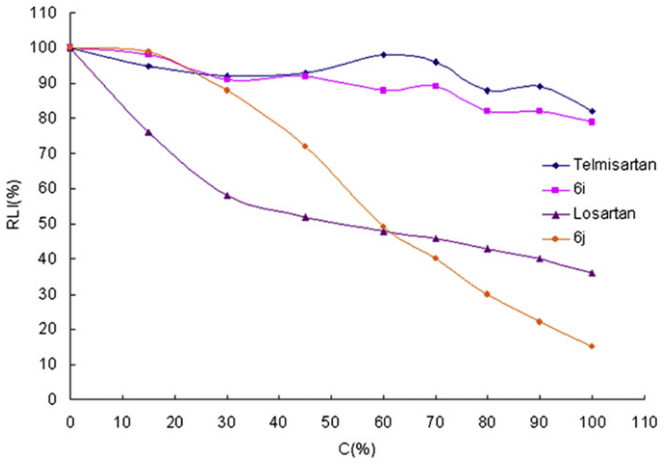


**Fig. 8.** Inhibition of compound **6i** and **6j** on photobacterium phosphoreum.

## Acknowledgments

Financial support of this work by the Fundamental Research Foundation of Beijing Institute of Technology (1050050320704) and the National Technological Project of the Manufacture and Innovation of Key New Drugs (2009ZX09103-143) was appreciated. We also thank Beijing Harmamatsu Photon Technique Inc. for the providing of the toxicity test instrument.

## Supplementary data

Supplementary data associated with this article can be found in the online version, at doi:10.1016/j.ejmech.2012.01.009. These data include MOL files and InChiKeys of the most important compounds described in this article.

## References

[1] B. Schmidt, B. Schieffer, Angiotensin II $AT_1$ receptor antagonists: clinical implications of active metabolites, J. Med. Chem. 46 (2003) 2261–2270.
[2] T.L. Goodfriend, M.E. Elliott, K.J. Catt, Drug therapy: angiotensin receptors and their antagonists, N. Engl. J. Med. 334 (1996) 1649–1655.
[3] G.K. .Aulakh, R.K. .Sodhi, M. Singh, An update on non-peptide angiotensin receptor antagonists and related RAAS modulators, Life Sci. 81 (2007) 615–639.
[4] J.D. Irvin, J.M. Viau, Safety profiles of the angiotensin converting enzyme inhibitors captopril and enalapril, Am. J. Med. 81 (suppl 4C) (1986) 46–50.
[5] Y. Lacourciere, J. Lefebvre, Cough induced by pharmacological modulation of the rennin-angiotensin-aldosterone system. Angiotensin converting enzyme inhibitors and angiotensin II receptor antagonists, in: N.S. Dhalla, P. Zahradka, I.M.C. Dixon, R.E. Beamish (Eds.), Angiotensin II Receptor Blockade: Physiological and Clinical Implications, Kluwer Academic publishers, Boston, 1998, pp. 115–125.
[6] M.A. Creager, L. Joseph, J.D. Victor, Vascular Medicine: A Companion to Braunwald's Heart Disease, Saunders, Philadelphia, 2006.
[7] Y. Furukawa, S. Kishimoto, K. Nishikawa, Hypotensive Imidazole Derivatives, U.S. 4340598, 1982.
[8] D.J. Carini, J.V. Duncia, P.E. Aldrich, A.T. Chiu, A.L. Johnson, M.E. Pierce, W.A. Price, J.B. Santella, G.J. Wells, R.R. Wexler, P.C. Wong, S.-E. Yoo, P.B.M.W.M. Timmermans, Nonpeptide angiotensin II receptor antagonists: the discovery of a series of *N*-(biphenylylmethyl)imidazoles as potent, orally active antihypertensives, J. Med. Chem. 34 (1991) 2525–2547.
[9] K. Kubo, Y. Kohara, E. Imamiya, Y. Sugiura, Y. Inada, Y. Furukawa, K. Nishikawa, T. Nakat, Nonpeptide angiotensin II receptor antagonists. Synthesis and biological activity of benzimidazole carboxylic acids, J. Med. Chem. 36 (1993) 2182–2195.
[10] U.J. Ries, G. Mihm, B. Narr, K.M. Hasselbach, H. Wittneben, M. Entzeroth, J.C.A. van Meel, W. Wienen, N.H. Hauel, 6-Substituted benzimidazoles as new nonpeptide angiotensin II receptor antagonists: synthesis, biological activity, and structure-activity relationships, J. Med. Chem. 36 (1993) 4040–4051.
[11] B. Ferrari, J. Taillades, P. Perreaut, C. Bernhart, J. Gougat, P. Guiraudou, C. Cazaubon, A. Roccon, D. Nisato, G. Le Fur, J.C. Brelière, Development of tetrazole bioisosteres in angiotensin II antagonists, Bioorg. Med. Chem. Lett. 4 (1994) 45–50.
[12] J.A. Brousil, J.M. Burke, Olmesartan medoxomil: an angiotensin II-receptor blocker, Clin. Ther. 25 (2003) 1041–1055.
[13] (a) A. Bali, Y. Bansal, M. Sugumaran, J.S. Saggu, P. Balakumar, G. Kaur, G. Bansal, A. Sharmac, M. Singh, Design, synthesis, and evaluation of novelly substituted benzimidazole compounds as angiotensin II receptor antagonists, Bioorg. Med. Chem. Lett. 15 (2005) 3962–3965;
(b) D.I. Shah, M. Sharma, Y. Bansal, G. Bansal, M. Singh, Angiotensin II $AT_1$ receptor antagonists: design, synthesis and evaluation of substituted carboxamido benzimidazole derivatives, Eur. J. Med. Chem. 43 (2008) 1808–1812;
(c) N. Kaur, A. Kaur, Y. Bansal, D.I. Shah, G. Bansal, M. Singh, Design, synthesis, and evaluation of 5-sulfamoyl benzimidazole derivatives as novel angiotensin II receptor antagonists, Bioorg. Med. Chem. 16 (2008) 10210–10215.
[14] W.-F. Yu, Z.-M. Zhi, H.-B. Zhu, L.-S. He, Synthesis of telmisartan and its derivatives and evaluation of their biological activities, Chin. J. Org. Chem. 36 (2006) 318–323.
[15] Full crystallographic details of **5e** have been deposited with the Cambridge Crystallographic Data Centre and allocated the deposition number CCDC 818973. Copies of the data can be obtained, free of charge, on application to The Director, CCDC, 12 Union Road, Cambridge CB2 1EZ, UK (Fax: +44 1223336 033; e-mail: deposit@ccdc.cam.ac.uk or www.ccdc.cam.ac.uk).
[16] H. .Yanagisawa, Y. Amemiya, T. Kanazaki, Y. Shimoji, K. Fujimoto, Y. Kitahara, T. Sada, M. Mizuno, M. Ikeda, S. Miyamoto, Y. Furukawa, H. Koike, Nonpeptide angiotensin II receptor antagonists: synthesis, biological activities, and structure–activity relationships of imidazole-5-carboxylic acids bearing alkyl, alkenyl, and hydroxyalkyl substituents at the 4-position and their related compounds, J. Med. Chem. 39 (1996) 323–338.
[17] A. Cappeli, C. Nannicini, A. Gallelli, G. Giuliani, S. Valenti, G.P. Mohr, M. Anzini, L. Mennuni, F. Ferrari, G. Caselli, A. Giordani, W. .Peris, F. Makovec, G. Giorgi, S. Vomero, Design, synthesis, and biological evaluation of $AT_1$ angiotensin II receptor antagonists based on the pyrazolo[3,4-b]pyridine and related heteroaromatic bicyclic systems, J. Med. Chem. 51 (2008) 2137–2146.
[18] K.M. Gough, K. Belohorcová, K. Kaiser, Quantitative structure–activity relationships (QSARs) of *Photobacterium phosphoreum* toxicity of nitrobenzene derivatives, Sci. Total Environ. 142 (1994) 179–190.
[19] Discovery Studio, 2.0 Version. Accelrys (2005).
[20] M.A.H. Ismail, S. Barker, D.A. Abou El Ella, K.A.M. Abouzid, R.A. Toubar, M.H. Todd, Design and synthesis of new tetrazolyl- and carboxy-biphenylylmethyl-quinazolin-4-one derivatives as Angiotensin II $AT_1$ Receptor Antagonists, J. Med. Chem. 49 (2006) 1526–1535.
[21] E.M. Krovat, T. Langer, Non-peptide angiotensin II receptor antagonists: chemical feature based pharmacophore identification, J. Med. Chem. 46 (2003) 716–726.
[22] H.-Y. Wang, L.-L. Li, Z.-X. Cao, S.-D. Luo, Y.-Q. Wei, S.-Y. Yang, A specific pharmacophore model of Aurora B kinase inhibitors and virtual screening studies based on it, Chem. Bio. Drug Des 73 (2009) 115–126.
[23] E.M. David, N.S. Tonous, K.P. Michael, A review of the structural and functional features of olmesartan medoxomil, an angiotensin receptor blocker, J. Cardiovasc. Pharmacol. 46 (2005) 585–593.
[24] Y. Kohara, K. Kubo, E. Imamiya, T. Wada, Y. Inada, T. Naka, Synthesis and angiotensin II receptor antagonistic activities of benzimidazole derivatives bearing acidic heterocycles as novel tetrazole bioisosteres, J. Med. Chem. 39 (1996) 5228–5235.
[25] (a) G.P. Mohr, A. Gallelli, M. Rizzo, M. Anzini, S. Vomero, L. Mennuni, F. Ferrari, F. Makovec, M.C. Menziani, P.G.D. Benedetti, G. Giorgi, Design, synthesis, structural studies, biological evaluation, and computational simulations of novel potent $AT_1$ angiotensin II receptor antagonists based on the 4-phenylquinoline structure, J. Med. Chem. 47 (2004) 2574–2586;
(b) A. Cappeli, G.P. Mohr, G. Giuliani, S. Galeazzi, M. Anzini, L. Mennuni, F. Ferrari, F. Makovec, E.M. Kleinrath, T. Langer, M. Valoti, G. Giorgi, S. Vomero, Further studies on imidazo[4,5-b]pyridine $AT_1$ angiotensin II receptor antagonists. Effects of the transformation of the 4-phenylquinoline backbone into 4-phenylisoquinolinone or 1-phenylindene scaffolds, J. Med. Chem. 49 (2006) 6451–6464.
[26] T. Tuccinardi, V. Calderone, S. Rapposelli, A. Martinelli, Proposal of a new binding orientation for non-peptide $AT_1$ antagonists: homology modeling, docking and three-dimensional quantitative structure-activity relationship analysis, J. Med. Chem. 49 (2006) 4305–4316.
[27] H. Sanderson, M. Thomsen, Comparative analysis of pharmaceuticals versus industrial chemicals acute aquatic toxicity classification according to the United Nations classification system for chemicals. Assessment of the (Q)SAR predictability of pharmaceuticals acute aquatic toxicity and their predominant acute toxic mode-of-action, Toxicol. Lett. 187 (2009) 84–93.
[28] M.J. Robertoson, M.P. Cunoosamy, K.L. Clark, Effects of peptidase inhibition on angiotensin receptor agonist and antagonist potency in rabbit isolated thoracic aorta, Br. J. Pharmacol. 106 (1992) 166–172.
[29] H.O. Schild, PA, A new scale for the measurement of drug antagonism, Br. J. Pharmacol. 2 (1947) 189–205.
[30] K. Kubo, Y. Inada, Y. Kohara, Y. Sugiura, M. Ojima, K. Itoh, Y. Furukawa, K. Nishikawa, T. Naka, Nonpeptide angiotensin II receptor antagonists. synthesis and biological activity of benzimidazoles, J. Med. Chem. 36 (1993) 1772–1784.
[31] H.A. Raul, Y.M.C. Violeta, P.M. Sandra, J.F. Francisco, A.F.S. Cesar, B. Victor, I.B. Hiram, S.Z.R. Luis, Molecular design and QSAR study of low acute toxicity biocides with 4,4′-dimorpholylmethane core obtained by microwave-assisted synthesis, Green Chem. 12 (2010) 1036–1048.